

# Evidence of a low temperature dynamical transition in concentrated PNIPAM microgels

Marco Zanatta,<sup>1</sup> Letizia Tavagnacco,<sup>2</sup> Elena Buratti,<sup>3</sup> Monica Bertoldo,<sup>3,\*</sup>

Francesca Natali,<sup>4</sup> Ester Chiessi,<sup>5</sup> Andrea Orecchini,<sup>6,†</sup> and Emanuela Zaccarelli<sup>2,‡</sup>

<sup>1</sup>*Department of Computer Science, University of Verona, Strada Le Grazie 15, 37138, Verona, Italy*

<sup>2</sup>*CNR-ISC and Department of Physics, Sapienza University of Rome, Piazzale A. Moro 2, 00185, Rome, Italy*

<sup>3</sup>*CNR-IPCF Istituto per i Processi Chimico-Fisici,*

*Sede Secondaria di Pisa, Consiglio Nazionale delle Ricerche,*

*Area della Ricerca, via G. Moruzzi 1, 56124 Pisa, Italy*

<sup>4</sup>*CNR-IOM, Operative Group in Grenoble (OGG), c/o Institut Laue Langevin,*

*6 rue Jules Horowitz, BP 156, 38042 Grenoble cedex 9, France*

<sup>5</sup>*Department of Chemical Sciences and Technologies,*

*University of Rome Tor Vergata, Via della Ricerca Scientifica I, 00133 Rome, Italy*

<sup>6</sup>*Department of Physics and Geology, University of Perugia and CNR-IOM, Via A. Pascoli, 06123, Perugia, Italy*

(Dated: June 12, 2025)

The occurrence of a dynamical transition at low temperature has been reported in a large number of different proteins. Here we provide the first observation of a “protein-like” dynamical transition in a non-biological aqueous environment. To this aim we exploit the popular colloidal system of poly-N-isopropylacrylamide (PNIPAM) microgels, extending their investigation to unprecedently high concentrations. Thanks to the heterogeneous polymeric architecture of the microgels, water crystallization is avoided in concentrated samples and we are thus able to monitor their atomic dynamics down to low temperatures. By elastic incoherent neutron scattering and molecular dynamics simulations, we find that a dynamical transition occurs at a temperature  $T_d \sim 250$  K. While the transition temperature is independent from PNIPAM mass fraction, its signature is smeared out on approaching dry conditions. The direct comparison between experiments and simulations shows quantitative agreement, providing evidence that the transition occurs simultaneously for PNIPAM and water dynamics. These findings are remarkably similar to what commonly observed in hydrated protein powders, suggesting that the dynamical transition is a generic feature in complex macromolecular systems, independently from their biological function.

Hydrated protein powders are known to undergo a so-called dynamical transition, which is associated to a sudden increase with temperature of the protein atomic mean-squared displacements (MSD). This is related to the onset of anharmonic motions which allow the protein to explore conformational substates corresponding to the structural configurations of functional relevance [1]. Thus, the transition is accompanied by the activation of the protein functionality, making it the subject of intensive research for its high relevance in the biological context. On the other hand, the dynamical transition is clearly distinct from the protein glass transition, the latter taking place at a lower temperature and involving other types of atomic motions [2]. Since its first observation in myoglobin [3], the dynamical transition has been reported for several proteins with different structures [2, 4] and in more complex biomolecules such as lipid bilayers [5] and DNA strands [6]. Although it appears to be closely related to biological functionality [7], some experiments have shown that the dynamical transition occurs also in unstructured proteins [8] and even in mixtures of unbound amino acids in aqueous environment [9]. Conversely, in dry biomolecules the transition

is suppressed, thus highlighting the prominent role of hydration water.

Recent studies have shown the dynamical transition to take place simultaneously for both protein and water dynamics [10, 11], thus lifting residual doubts on the close dynamical coupling between hydration water and biomolecules [12–14]. Altogether, these evidences put forward the hypothesis that water plays a driving role in the dynamical transition and thus suggest that this phenomenon may be ubiquitous in the context of hydrated systems. This opens up the possibility to investigate also non-biological systems, for example synthetic macromolecules, to shed light on the nature of the transition and to unveil the role of water. To this aim, it is particularly important to focus on complex macromolecular environments which could, on one hand, mimic the multi-faceted potential energy landscape of proteins and, on the other hand, avoid water crystallization and allow the investigation of atomic dynamics at low temperatures. These conditions can be achieved by using the peculiar characteristics of microgel particles [15]. Microgels are colloids made by crosslinked polymer networks with a heterogeneous structure composed of a dense core and a loose corona [16]. Such a complex internal architecture appears to be particularly suitable to prevent water nucleation. Here we focus on the most studied type of microgels, which are made of poly-N-isopropyl-acrylamide

\* monica.bertoldo@pi.ipcf.cnr.it

† andrea.orecchini@unipg.it

‡ emanuela.zaccarelli@cnr.it

(PNIPAM), a thermoresponsive polymer that is soluble in water at room temperature and below. As PNIPAM and proteins are both polyamides, they both interact via hydrogen bonding with water, which reinforces the idea of hydrated PNIPAM as a promising model to mimic protein-water systems.

PNIPAM microgels have been so far extensively studied around ambient temperature as a tunable model system for elucidating phase transitions and glassy behavior [17]. We now extend their investigation to a yet unexplored region of phase diagram, encompassing PNIPAM mass fractions (wt) in the range  $43 \leq c \leq 95\%$ wt and a wide range of temperatures, namely  $152 \lesssim T \lesssim 287$  K. By combining elastic incoherent neutron scattering (EINS) experiments with all-atom molecular dynamics (MD) simulations, we probe the internal dynamics of microgels at short time and length scales. We find that our suspensions do not crystallize for PNIPAM mass fractions  $\gtrsim 43\%$ wt at any temperature, in good agreement with calorimetric data on PNIPAM chains [18, 19]. Most crucially, we find the occurrence of a “dynamical” transition at  $T_d \approx 250$  K, akin to that observed in proteins. Indeed, the value of the transition temperature does not depend on PNIPAM mass fraction, but the transition tends to disappear when approaching dry conditions. We directly compare the measured EINS intensities and their associated MSD with those calculated in simulations, finding quantitative agreement between the two. Moreover, simulations show a strong coupling for both PNIPAM and water dynamics, for which a discontinuity in diffusional dynamics occurs at the same temperature. These results represent, to our knowledge, the first observation of a genuine dynamical transition in a non-biological aqueous system, providing generality for the concept of a low-temperature dynamical transition in disordered macromolecules with internal degrees of freedom.

## RESULTS

### EINS experiments

EINS experiments were performed on hydrogenated PNIPAM microgels in  $D_2O$  at five PNIPAM mass fractions between 43% and 95% [20]. In thermal neutron scattering, the incoherent cross-section of hydrogen atoms is more than an order of magnitude larger than both coherent and incoherent cross-sections of the other atomic species in our PNIPAM suspensions. Therefore, the incoherent signal of the hydrogenated PNIPAM network dominates the mostly coherent signal of deuterated water, providing selective access to the microscopic dynamics of the polymer matrix.

EINS data were collected at the backscattering spectrometer IN13 of the Institut Laue-Langevin (ILL, Grenoble, France). IN13 has an energy-resolution  $\Delta E = 8 \mu\text{eV}$  (FWHM) and covers a momentum transfer interval

from 0.3 to  $4.5 \text{ \AA}^{-1}$ , thus accessing motions faster than about 150 ps taking place in a spatial region between 1 and 20  $\text{\AA}$ . In this way, we essentially probe the internal dynamics of the microgel and its behavior on the atomic scale. This is important because, even though our samples are glassy on the colloidal scale [21, 22], the volume fraction occupied by the microgels is still much lower than that of the polymer glass transition[18], so that we can safely assume that the polymeric degrees of freedom are in equilibrium. Indeed our results confirm this assumption, as they show a progressive and smooth behavior with PNIPAM mass fraction, are reproducible with respect to sample preparation and are fully reversible in temperature.

The measured incoherent elastic intensities  $I(Q, 0)$  as a function of temperature and momentum transfer  $Q$  are reported in Fig.1(a) for selected samples with PNIPAM mass fraction of 43% and 60%. Data were recorded under thermal cycles of cooling (upper panels) and heating (lower panels) in a range of temperatures between 287 K and 152 K. The temperature behaviour is best observed in the  $Q$ -integral of  $I(Q, 0)$ , reported in Fig. 1(b). Upon cooling, the integrated EINS intensity progressively increases until a sharp variation occurs at a characteristic “dynamical transition” temperature  $T_d \sim 250$  K, below which the intensity increase continues with a smaller but linear slope. Such a discontinuity is more pronounced at the lowest PNIPAM concentration and gradually disappears with decreasing water content. Upon heating back, the measured data fall on top of the corresponding ones at the same  $T$ , confirming the full reversibility of the process.

At each temperature, the average atomic MSD can be calculated from the  $Q$ -dependence of  $I(Q, 0)$ . To this end, the EINS data  $I(Q, 0)$  were fitted with a double-well model, that captures the data behavior very well (see SI, Fig. S1 and S2). The resulting MSDs in Fig. 1(c) reflect the discontinuity observed in the  $Q$ -integrated intensity at  $T_d \sim 250$  K. Below  $T_d$ , the linear temperature evolution of the MSD is typical of a harmonic solid. Conversely, the sudden slope increase above  $T_d$  witnesses an enhanced mobility of the PNIPAM atoms, due to the onset of anharmonic motions and resulting in the corresponding elastic intensity drop.

It is worth noting that the observed discontinuity at  $T_d$  might be attributed to an underlying crystallization process associated to the  $D_2O$ . However, the measured  $I(Q, 0)$  for pure  $D_2O$  in the same temperature range shows defined crystalline peaks that do not appear in low- $T$  PNIPAM suspensions (see SI, Fig. S3). This suggests that the elastic intensity drop of the PNIPAM network originates from a mechanism other than water crystallization.

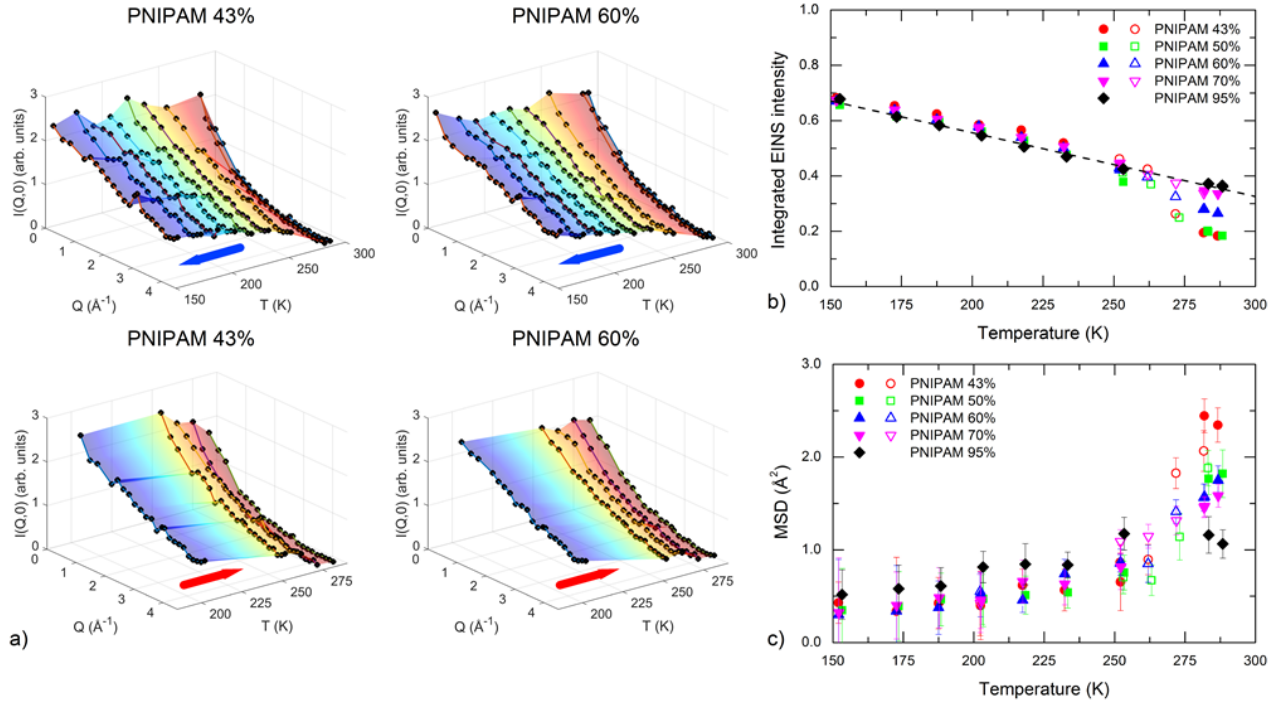


FIG. 1. EINS data. a) Incoherent elastic intensities  $I(Q, 0)$  measured on PNIPAM microgels in  $\text{D}_2\text{O}$  with a mass fraction concentration of 43% and 60% as a function of temperature  $T$ . Top (bottom) panels reports data recorded under cooling (heating). b) Integral over  $Q$  of  $I(Q, 0)$  as a function of  $T$ . The integrated EINS intensities are normalized to 1 for  $T \rightarrow 0$ . c) Temperature evolution of MSD as obtained using the double-well model (see SI). In b) and c) measurements under cooling are presented with filled symbols whereas those under heating with open symbols.

### MD Simulations

To identify the microscopic mechanism responsible for the observed change in PNIPAM dynamics taking place at  $T_d$ , we rely on all-atom MD simulations. To this aim, we designed a new microgel model (described in Materials and Methods and SI) and performed its numerical investigation at mass fractions of 40% and 60%. A snapshot of the *in silico* microgel is displayed in Fig. 2(a). The PNIPAM network was built with a crosslinker/monomer ratio of 1/28 which, taking into account the inhomogeneous density of a PNIPAM particle, describes an inner region (e.g. the core region) of the microgel. The number of water molecules per monomeric unit is smaller than the experimentally determined value of hydration molecules for PNIPAM microgels [23] for both concentrations. Thus, we can safely assume that all water molecules in the simulations are hydration water and not bulk water.

At each studied temperature, we monitored the dynamics of both microgel and water atoms separately. To characterize microgel dynamics we calculated the self intermediate scattering function (SISF) which probes the single-particle translational dynamics at a characteristic wavevector. Fig. 2(b) displays the SISFs calculated for the hydrogen atoms of PNIPAM 40%wt at  $Q = 2.25 \text{ \AA}^{-1}$ , i.e. at the position of the first peak in the oxygen-oxygen structure factor of bulk water [24]. PNIPAM internal

dynamics exhibits a two-step behavior typical of glass-forming liquids: an initial fast relaxation is followed by a long-time, slow relaxation indicating structural rearrangement. At the lowest studied temperatures, the SISFs do not decay completely to zero, an indication that the system is becoming arrested on the considered time window. However, studies on longer timescales reveal that aging phenomena do not play a major role at the studied temperatures (see SI, Figs. S5 and S6). The long-time relaxation of the SISFs is well described by a stretched exponential as in standard glass-formers, thus providing an estimate of the structural relaxation time  $\tau_p$ . This is shown in Fig. 3(a) as a function of temperature in an Arrhenius plot. We find that  $\tau_p$  obeys two distinct dynamical regimes, each characterized by an Arrhenius dependence. The crossover temperature of about 250 K is strikingly similar to that found in EINS experiments. The activation energies are  $28.4 \pm 0.8 \text{ kJ mol}^{-1}$  and  $14.5 \pm 0.5 \text{ kJ mol}^{-1}$  for the high and low temperature regime, respectively.

To complement these results, we also investigated the hydration water dynamics by looking at the MSD of the oxygen atoms, see Fig. 2(c). Similarly to PNIPAM SISFs, we observe a slowing down of water dynamics with decreasing  $T$ . While at high  $T$  the MSD shows a diffusive behavior in the studied time interval, upon lowering temperature the onset of an intermediate plateau is observed.

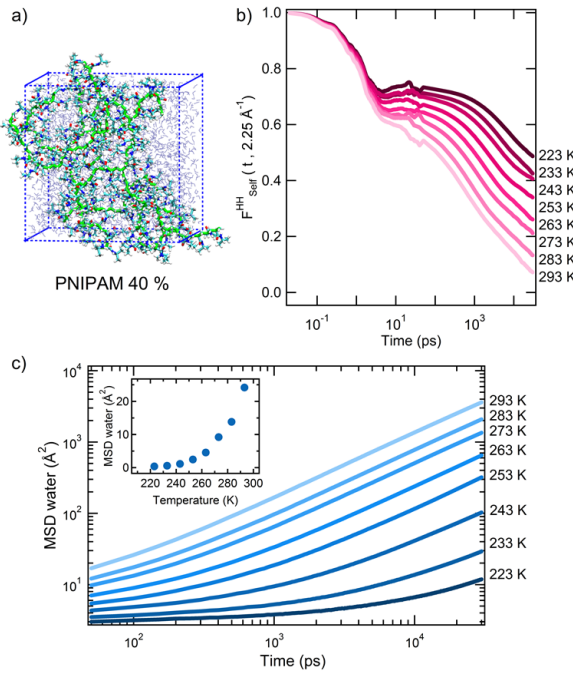


FIG. 2. MD simulation results for 40% mass fraction. a) Snapshot of the simulated PNIPAM microgel. Chain atoms are displayed in green to highlight the network structure. b) Self-intermediate scattering function of PNIPAM hydrogen atoms calculated at  $Q = 2.25 \text{ \AA}^{-1}$  as a function of temperature. c) Time-evolution of the mean square displacements of water molecules. The inset shows the water mean square displacements values at 150 ps as a function of  $T$ .

This is a characteristic feature of glassy systems, indicating that atoms remain trapped in cages of nearest neighbours for a transient, before eventually diffusing away at long times. Water oxygen atoms retain a diffusive behavior at all studied  $T$ , so that it is possible to estimate their self-diffusion coefficient  $D_w$ . This is also reported in the Arrhenius plot of Fig. 3(a), where  $D_w$  is also found to follow two distinct Arrhenius regimes, crossing again at a temperature  $\approx 250$  K. Furthermore, in the inset of Fig. 2(c) the water MSD calculated at a time of 150 ps, matching the experimental time resolution, is reported as a function of  $T$ . A clear increase of the MSD is found above  $\sim 250$  K. This strikingly matches the MSD behavior observed by EINS in our PNIPAM samples and is closely reminiscent of other experimental and simulation results on protein hydration water [10, 11, 25–27].

To make a closer connection to protein dynamics, we calculated the root mean square fluctuation (RMSF) of PNIPAM hydrogen atoms, which measures the fluctuations of the atom positions with respect to the averaged structure over a defined period of time. We monitored this quantity separately for hydrogen atoms of the methyl groups and those of the backbone. The evolution with temperature of the RMSF for both types of hydrogen atoms, averaged over the experimental resolution time, is shown in Fig. 3(b). Again, a clear change

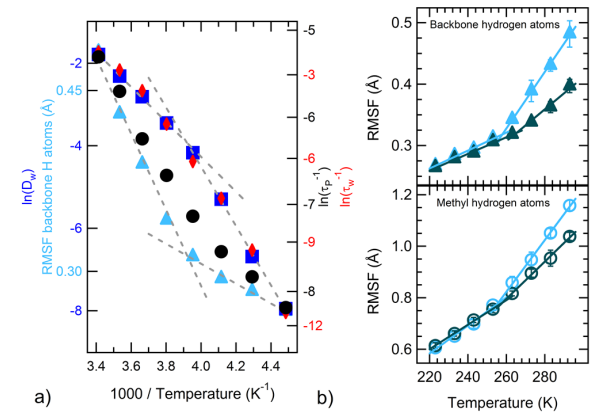


FIG. 3. Water-PNIPAM coupling. a) Temperature dependence of water diffusion coefficient (squares); SISF relaxation times for PNIPAM hydrogen atoms (circles) and water oxygen atoms (diamonds); root mean square fluctuation (RMSF) of backbone hydrogen atoms (triangles) calculated from MD simulations. Dashed lines are guides to the eye. b) Temperature evolution of RMSF of the PNIPAM hydrogen atoms for 40% wt (light blue) and for 60% wt (dark green) averaged over 150 ps: methyl groups (circles), backbone atoms (triangles).

is detected at a temperature  $\sim 250$  K for both types of atoms with a stronger effect for the backbone hydrogen atoms. Such a change is observed for both studied mass fractions, suggesting that concentration does not play any role on the value of the crossover temperature, for both water and PNIPAM atoms, but it only smears out the variation, making the two regimes progressively similar to each other. These findings are in agreement with the concentration dependence of the experimental  $I(Q, 0)$  (Fig. 1(b)). Fig. 3(a) summarizes the MD results, showing that  $\tau_p$ , the RMSF of PNIPAM backbone atoms, the self-diffusion constant of water and the associated relaxation time  $\tau_w$  all display a clear change at  $T \sim 250$  K, a temperature strikingly similar to the one where the EINS data reveal a variation. Thus, simulations clearly show that the dynamical properties of both PNIPAM and water are slaved to each other.

These results suggest to interpret the transition observed at  $T_d$  as the analogue of the protein dynamical transition for PNIPAM microgels suspensions. Indeed, several features are shared by protein and PNIPAM dynamical transition: (i)  $T_d$  does not depend on the concentration and the transition vanishes for dry conditions; (ii) the transition takes place at a temperature higher than that of the glass transition [2]; (iii) the strong coupling between water and PNIPAM dynamics, reported in Fig. 3(a), is well established in hydrated proteins [10, 12–14].

It is then natural to ask whether water drives the occurrence of such dynamical transition, being ubiquitous in proteins and in PNIPAM microgels suspensions. To partially answer this question, we refer to recent simulation studies on confined water, that have provided a

detailed characterization of slow dynamics in water [28]. In particular the study of hydrated lysozyme [29] has identified a new (long) timescale governing the behavior of confined water, which is characterized by two distinct Arrhenius regimes, in full analogy with the present findings for water confined in microgels. Such a behavior was interpreted as a strong-strong transition due to the coupling of hydration water with the fluctuations of the protein structure and found to occur in correspondence to the protein dynamical transition. The same correspondence is found in our simulations, suggesting that indeed hydration water drives the dynamical transition. In support of this idea comes the fact that the behavior with concentration is similar for both PNIPAM microgels and hydrated proteins.

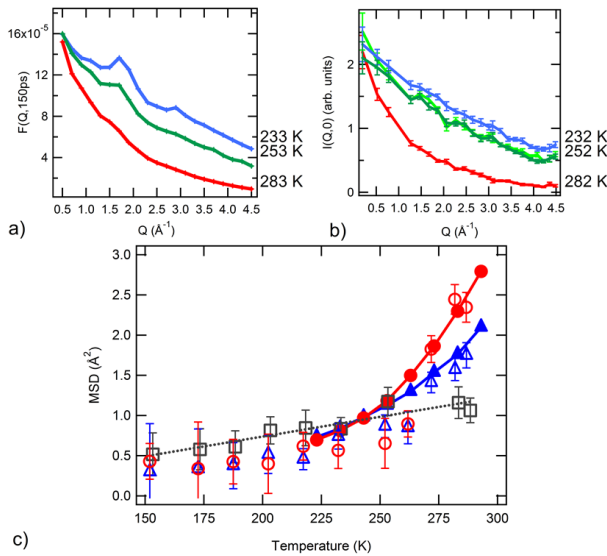


FIG. 4. Quantitative comparison between experiments and simulations. a) Neutron spectra as a function of temperature as calculated from the MD simulations of the PNIPAM microgel at 40%. The total intermediate scattering functions are displayed at a value of 150 ps for comparison with the experimental data. b) EINS spectra measured on the sample with a PNIPAM concentration of 43% as a function of temperature. Data shown at 252 K compare the spectra measured under cooling (dark green) and heating (green). c) Temperature dependence of experimental (open symbols) MSD for PNIPAM mass fractions 43% (circles), 60% (squares) and 95% (triangles) and numerical (filled symbols) MSD, calculated at 150 ps for PNIPAM hydrogen atoms only, for PNIPAM mass fractions 40% (circles) and 60% (squares). The dashed line is a guide to the eye suggesting a linear behavior for the dry sample, for which the dynamical transition is suppressed.

#### Comparison between MD simulations and EINS data

We now provide a direct comparison between experimental and numerical data. To this end, we have calculated the elastic intensity in simulations, as explained

in SI. The resulting  $I(Q, 0)$  as a function of  $Q$  are reported in Fig. 4 for simulations (a) and experiments (b) at corresponding temperatures for the 40%wt sample. The data are in very good qualitative agreement, also showing the presence of more pronounced peaks at comparable wavevectors. From the simulated trajectories we can also calculate the MSD of the PNIPAM hydrogen atoms and compare them with those resulting from the fit of the experimental  $I(Q, 0)$ . The comparison is shown in Fig. 4(c). The numerical MSD are in striking quantitative agreement with the experimental ones, without need of any scaling factor.

## DISCUSSION AND CONCLUSIONS

In this work we have reported evidence of the occurrence of a dynamical transition in concentrated PNIPAM microgels suspensions at low temperatures, akin to that observed in proteins. We have combined EINS measurements with atomistic MD simulations, based on a new model specifically developed to mimic the interior of a microgel network. While a detailed numerical representation of a whole microgel is currently unfeasible, our study is capable to resolve the intra-network dynamics of PNIPAM atoms at the short timescales probed by EINS experiments. Thanks to the use of highly concentrated samples, we have extended the investigation of microgel suspensions to unprecedentedly low temperatures, avoiding water crystallization. Our findings are in agreement with calorimetric data for linear PNIPAM chains, showing that crystallization is absent for polymer mass fractions above  $\sim 50\%$  [18, 19]. These results open up the possibility to systematically investigate very high concentration and low temperature microgel samples beyond current practice.

The dual colloidal/polymeric nature of microgels [30] bridges the properties of classical hard-sphere colloids and soft polymeric particles [31], allowing for the presence of two distinct glass transitions on the colloidal and the polymeric scale, respectively. Both transitions depend on temperature, given the thermoresponsive character of PNIPAM, which is responsible for the so-called Volume Phase Transition at  $T_{VPT} \sim 305$  K, from a swollen state of the microgel particles for  $T \lesssim T_{VPT}$  to a collapsed state above it. In the swollen regime, a colloidal glass transition takes place at a PNIPAM mass fraction of about  $\sim 10\%$ wt [22]. Although very few studies of microgels at high concentrations exist, we can expect the glass transition on the polymeric scale to be similar to that reported for PNIPAM chains, amounting to about 80%wt at ambient temperature [18, 19]. This means that, for the concentrations studied in this work, the microgel samples are macroscopically arrested in a glass-like state. A legitimate question thus concerns the reproducibility of our samples and their stability. We have shown that a careful preparation and measurement protocol allowed us to obtain homogeneous samples (see Materials and

Methods), ensuring a complete reproducibility of the results and a smooth, progressive variation with microgel concentration of the dynamical observables at the investigated short time and length scales.

The study of microgels in water at low temperatures poses a numerical challenge in appropriately identifying a suitable water model, able to realistically describe its peculiar behavior. Very accurate models exist which are usually able to describe specific aspects. In particular TIP4P/ICE was devised to accurately reproduce the solid properties of water [32]. We have chosen to work with this model because it reproduces water melting at  $\sim 270$  K, much closer to reality than the  $\approx 250$  K predicted by the mostly adopted TIP4P/2005 [33]. Thus, it should be more realistic also in describing supercooled water environments. Our results confirm this hypothesis, providing quantitative agreement with experiments in the investigated  $T$ -range for the dynamical properties of PNIPAM atoms. It will be interesting to test other models under the same conditions, particularly TIP4P/2005, as well as to extend our studies at higher temperatures.

The similarity of the transition reported here for hydrated PNIPAM microgels with that commonly observed in proteins could be important to better understand the microscopic origin of such a transition. Indeed, there are still controversial aspects in the literature, particularly concerning the role played by water. Two experimental studies have recently proposed an alternative picture for the dynamical transition, which would support the view that a transition may occur independently from the presence of water. Liu and coworkers reported the observation of a dynamical transition also in dry deuterated proteins [34], mainly due to backbone heavy atoms. While the relevance of the traditional transition in hydrated proteins remains unaltered, the role of such “dry” transition is still uncertain. It might provide one of the contributions to flexibility involved in biological processes, although in most proteins full functionality is achieved in the hydrated state only. In addition, Mamontov and coworkers investigated a simple polymeric system in non-aqueous environment [35], claiming to observe a dynamical transition similar to the protein one. However, in the latter study the temperature of the transition significantly depends on polymer concentration, differently to what found here and for hydrated protein studies, suggesting that its microscopic nature could be different.

We found that microgels are extremely efficient in confining water, because the lower limit of sample crystallization is close to 40% PNIPAM mass fraction, a value that exceeds in amount of water what commonly found in other confining environments. Indeed, the typical protein concentration where crystallization is avoided is  $\approx 60\%$  in protein mass fraction [3, 10, 11, 36]. Thus, our study suggests that stable samples with a majority of water can be studied down to very low temperatures, which could be of potential interest for the investigation of liquid-like water behavior in the so-called no man’s land region of the phase diagram. The efficient confinement role played

by microgels is probably due to their intrinsic network disorder and to their inhomogeneous internal architecture. It would be interesting to investigate the occurrence of a dynamical transition in other macromolecular environments that could also be appropriate for suppressing water crystallization.

As a whole, our results strongly suggest that the dynamical transition is a generic feature of water hydrating complex macromolecular suspensions with biological and non-biological implications. This work also puts forward colloidal microgels as excellent models for a deeper understanding of the functional relevance of protein dynamical transition. In proteins, an energy landscape endowed with a large number of conformational states, each containing several tiers of substates, is considered of essential biological importance, as proteins could not function without such a reservoir of entropy [1]. Likewise, the occurrence of a protein-like dynamical transition in PNIPAM microgels might well be ascribed to a similarly rich amount of conformational substates, due to the particularly complex and multi-scaled architecture of the polymer network.

## MATERIAL AND METHODS

### Sample preparation

Microgels have been synthesized by precipitation polymerization at  $T = 343$  K of N-isopropylacrylamide (NIPAM) in water (0.136 M) in the presence of N,N'-methylenebisacrylamide (BIS)(1.82 mM). The reaction was carried out in presence of 7.80 mM sodium dodecylsulfate as surfactant and potassium persulfate (2.44 mM) as radical initiator. The reaction was carried out for 10 h in nitrogen atmosphere. The obtained colloidal dispersion was purified by exhaustive dialysis against pure water, lyophilized, dispersed in D<sub>2</sub>O, lyophilized and dispersed again in D<sub>2</sub>O to a final concentration of 10%. The obtained microgels have been characterized by dynamic light scattering (Zetasizer Nano S, Malvern) and the hydrodynamic diameter was found to be  $94 \pm 3$  nm at 293 K with a size polydispersity of  $0.17 \pm 0.01$  nm.

### EINS experiments

EINS experiments were carried out on PNIPAM microgel suspensions with a PNIPAM mass fraction of 43%, 50%, 60%, 70%, and 95% (dry sample). To single out the incoherent signal from PNIPAM hydrogen atoms samples were prepared in D<sub>2</sub>O. Measurements were performed at the backscattering spectrometer IN13 of the Institut Laue-Langevin (ILL, Grenoble, France). PNIPAM samples were measured inside flat aluminum cells (3.0  $\times$  4.0 cm), sealed with an In o-ring. The thickness of the cell was adjusted to achieve a transmission of about 88% for each sample. Samples at the required

concentrations were obtained by filling sample holders with PNIPAM dispersion at 10% and by allowing the exceeding D<sub>2</sub>O evaporating at room temperature under vacuum. Once the desired concentration was reached, holders were sealed and samples were left to homogenize for not less than four days. EINS data were acquired in the fixed-window elastic mode, thus collecting the intensity elastically scattered as a function of  $Q$ . Data were corrected to take into account incident flux, cell scattering, and self-shielding. The intensity of each sample was normalized with respect to a vanadium standard to account for the detector efficiency. Multiple scattering processes have been neglected.

### PNIPAM model and MD Simulations

The model mimics, with an atomic detail, a cubic portion of PNIPAM microgel for a polymer mass fraction of 40 and 60%wt. The macromolecular network, modelled as isotropic, includes 12 atactic PNIPAM chains jointed by 6 4-fold bisacrylamide crosslinks (see Figure S4). Amide groups of PNIPAM residues are represented in the trans conformation. The 3-D percolation of the polymer scaffold is accounted by the covalent connectivity between adjacent periodic images. The number average molecular weight of chains between crosslinks,  $M_c$ , is 1584 g/mol, with a polydispersity index of 1.02 and an average degree of polymerization of 14. Taking into account the NIPAM/BIS feed ratio used in the synthesis and the non-uniform crosslink density of PNIPAM microgels, the model represents a region in proximity to the core-shell boundary of the particle. MD simulations of PNIPAM microgels were carried out at 8 temperatures (from 293 K to 223 K every 10 K). A trajectory interval of about 0.5  $\mu$ s was calculated for each temperature. Additional details are given in the SI.

### ACKNOWLEDGMENTS

MZ, LT and EB equally contributed to this work. LT, MB, EC and EZ acknowledge support from European Research Council (ERC-CoG-2015, Grant No. 681597 MIMIC), MB, AO and EZ from MIUR-PRIN. We acknowledge ILL for beamtime and CINECA-ISCRA for computer time.

## SUPPORTING INFORMATION

### Preparation and stability of the samples for EINS measurements

To obtain samples with the required PNIPAM concentration within the cell employed at IN13, we started from the prepared microgel dispersion at 10%. We then proceeded by evaporation of the exceeding D<sub>2</sub>O in dry atmosphere, using a desiccator under moderate vacuum ( $\sim 10$  mmHg). Once reached the final concentration, cells were sealed and left to homogenize at room temperature for at least four days before analysis. The sample at 95% composition was prepared from film casting the PNIPAM dispersion at 10% up to dryness in Petri dish. The obtained transparent films were milled with an IKA MF 10.1. Cutting-grinding give rise to a rough powder that was poured into an aluminum cell for neutron scattering. It is important to note that, after EINS measurements were performed, cells were opened and no changes in the samples morphology were detected, showing a homogeneous character and no compartmentalization effects.

### EINS measurement and data analysis

In the incoherent approximation, the elastic neutron scattering intensity  $I(Q, 0)$  can be described by the double-well model [3]. Within this approximation, hydrogen atoms are supposed to be dynamically equivalent and may jump between two distinct sites of different free energy. The elastic intensity can be thus written as:

$$I(Q, 0) = \exp(-Q^2 \langle \Delta u^2 \rangle_{vib}) \left[ 1 - 2p_1 p_2 \left( 1 - \frac{\sin(Qd)}{Qd} \right) \right] \quad (1)$$

where  $p_1$  and  $p_2$  are the probabilities of finding the hydrogen atom, respectively, in the ground and excited state,  $\langle \Delta u^2 \rangle_{vib}$  corresponds to the vibrational mean square displacement of protons rattling in the bottom of the wells, and  $d$  is the distance between the two wells. In this model, where a transition between the two states represents a jump between conformational substates in the free energy surface, the amplitude of the 3-dimensional structural fluctuations is given by the relationship [37]:

$$\langle \Delta r^2 \rangle = -6 \left( \frac{d \ln I(Q)}{dQ^2} \right)_{Q=0} = 6 \langle \Delta x^2 \rangle_{vib} + 2p_1 p_2 d^2 \quad (2)$$

Typical examples of the fits to the data with Eq. 1 are shown in Figs. S1 and S2 respectively for 43% and 60% samples. A pure D<sub>2</sub>O sample was also measured to completely rule out the possibility of its crystallization in PNIPAM samples. Fig. S3 shows the  $I(Q, 0)$  for heavy water and for PNIPAM 43% and 60% at 153 K. PNIPAM samples do not show any traces of the D<sub>2</sub>O Bragg peaks.

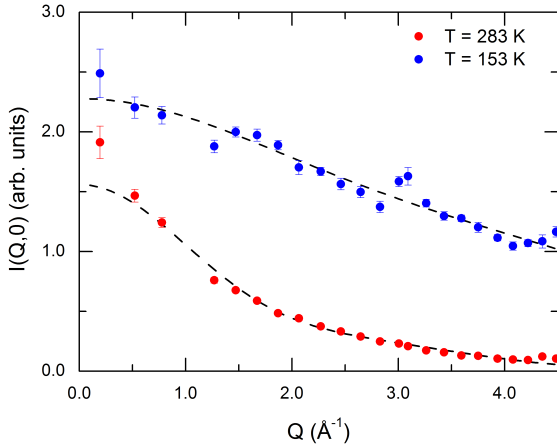


FIG. S1.  $I(Q,0)$  measured on the PNIPAM 43% sample at 283 K (red dots) and 153 K (blue dots); the black dashed line is the fit using Eq. 1.

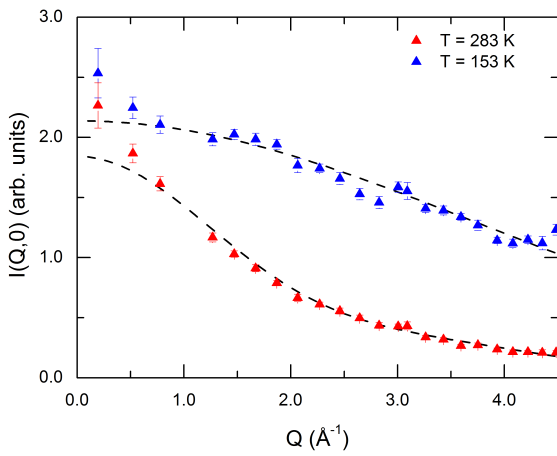


FIG. S2.  $I(Q,0)$  measured on the PNIPAM 60% sample at 283 K (red dots) and 153 K (blue dots); the black dashed line is the fit using Eq. 1.

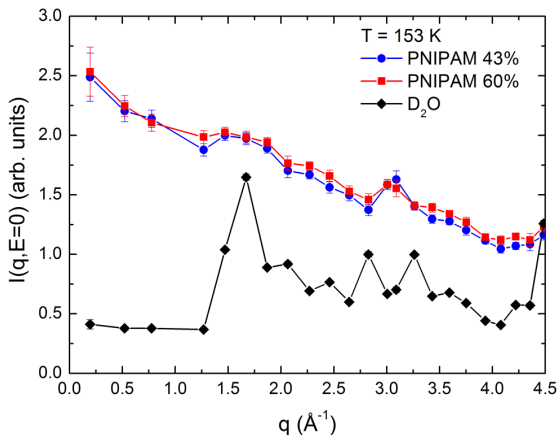


FIG. S3.  $I(Q,0)$  measured on pure  $D_2O$  compared with that obtained on PNIPAM 43% and 60% at 153 K.

## PNIPAM model development

An isotropic polymer scaffold, with the network topology shown in Fig. S4, was built by cross-linking atactic PNIPAM chains in the minimum energy conformation[38]. Amide groups of PNIPAM residues are modeled in the trans conformation. Extra-boundaries covalent connectivity between polymer chains was applied. The network model includes 6 4-fold bisacrylamide junctions and has a number average molecular weight of chains between cross-links,  $M_c$ , of 1584 g/mol, with a polydispersity index of 1.02. The average degree of polymerization of chains between junctions is  $14 \pm 2$ . The polymer scaffold was hydrated by a shell of water molecules to set the PNIPAM concentration in the microgel. Then the system was equilibrated at 293 K in a pressure bath at 1 bar up to a constant density value, i.e. tot-drift less than  $2 \times 10^{-3}$  g cm<sup>-3</sup> over 20 ns. A similar equilibration procedure was applied at each temperature before the NVT run.

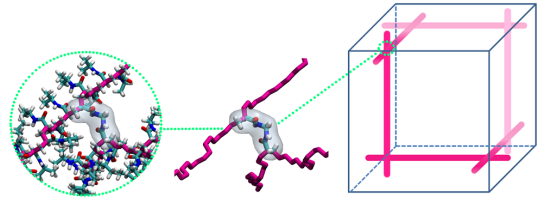


FIG. S4. Schematic representation of the microgel network model.

## MD simulations procedure

Molecular dynamics simulations of PNIPAM microgels were carried out using the GROMACS 5.0.4 software[39, 40]. The polymer network was modeled using the OPLS-AA force field [41] with the implementation by Siu et al. [42], while water was described with the Tip4p/ICE model[32]. The system was equilibrated for 120 ns for  $T \geq 273$  K and for 320 ns for  $T \leq 263$  K in the NPT ensemble, taking into account the longer equilibration time needed at lower temperatures. Simulation data were collected for 330 ns in the NVT ensemble, with a sampling of 0.2 frame/ps. The leapfrog integration algorithm was employed with a time step of 0.2 fs, cubic periodic boundary conditions, and minimum image convention. The length of bonds involving hydrogen atoms was kept fixed with the LINCS algorithm. The temperature was controlled with the velocity rescaling thermostat coupling algorithm with a time constant of 0.1 ps. Electrostatic interactions were treated with the smooth particle-mesh Ewald method with a cutoff of non-bonded interactions of 1 nm. The last 100 ns of trajectory were considered for analysis. The software MDANSE [43] as well as in-

house codes were used for analysis of MD simulations to be compared with the neutron scattering data. Trajectory format manipulations (or conversions) were carried out by the software WORDOM [44]. The software VMD [45] was employed for graphical visualization.

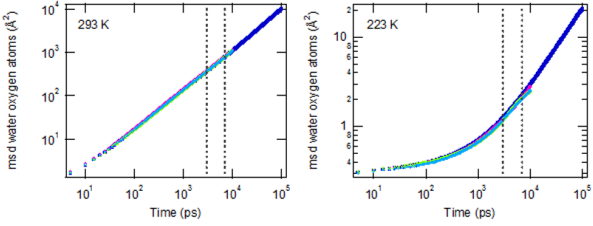


FIG. S5. Comparison between the mean square displacements of water oxygen atoms at 293 K (left panel) and 223 K (right panel) as calculated from the MD simulations over 100 ns of trajectory (blu squares), 0-10 ns (pink diamonds), 50-60 ns (green triangles) and 90-100 ns (light blue circles). Dashed lines highlight the linear region used for water diffusion coefficient calculation.

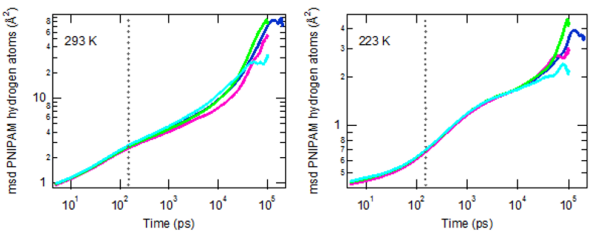


FIG. S6. Comparison between the mean square displacements of PNIPAM hydrogen atoms at 293 K (left panel) and 223 K (right panel) as calculated from the MD simulations over 200 ns of trajectory (blu lines), 0-100 ns (pink lines), 50-150 ns (green lines) and 100-200 ns (light blue lines). The value at the experimental time resolution of 150 ps is indicated with a dashed line.

### Reproducibility of numerical results

The numerical data are not affected by aging dynamics on the timescales investigated in the manuscript. To show that this is the case we report the evolution of the MSD upon changing the time interval for the calculation as well as waiting time  $t_w$ . Fig. S5 shows the MSD of water oxygen atoms at the highest ( $T = 293\text{K}$ ) and lowest ( $T = 223\text{ K}$ ) investigated temperatures. We calculate the MSD for a total time of 100 ns and compare it to the corresponding one calculated for only 10 ns (as used in the manuscript, Fig.2(c)). In addition, we also calculate it for  $t_w = 0, 50, 90$  ns. All curves superimpose on the entire investigated timescale, in particular for the intermediate window where the self-diffusion coefficient was extracted,

indicated by vertical dashed lines. This behaviour holds for both high and low temperatures. Similarly, Fig. S6 shows the MSD of PNIPAM hydrogen atoms at the same two temperatures over a total interval of 100 and 200 ns, the former being the ones from which we extract the value at 150 ps, reported in the manuscript in Fig. 4c. We also calculate it for waiting times  $t_w = 0, 50, 100\text{ns}$ . At long times, some differences, that are mostly attributable to statistical error rather than aging, are visible. However, it is clear that for the timescale of relevance for comparison with experimental data, i.e. 150 ps, indicated by a vertical dashed line, no significant aging effects are found. This analysis ensures that the numerical data are reproducible and the system is well equilibrated for the short timescales studied in this work.

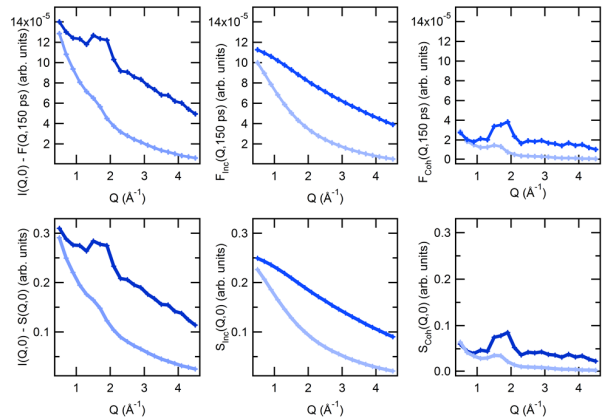


FIG. S7. Comparison between simulated neutron spectra  $I(Q, 0)$  calculated from the intermediate scattering functions at the experimental time resolution of 150 ps (upper panels) and from the total dynamical structure factors convoluted with the experimental resolution (lower panels) at 223 K (blue lines) and 293 K (light blue lines). The incoherent  $F_{Inc}$  and  $S_{Inc}$  are reported in the central panels of each row, while the coherent  $F_{Coh}$  and  $S_{Coh}$  contributions are shown in the rightmost panels.

### Calculation of $I(Q)$ from numerical simulations

We have calculated both the coherent and incoherent intermediate scattering functions for all atoms in the simulations for wavevectors in the range  $0.3 \leq Q \leq 4.5 \text{ Å}^{-1}$ . By summing the two contributions, weighted by the appropriate scattering lengths and by the partial concentrations, we have obtained the full differential cross-section. Its value at the experimental time resolution of 150 ps provides the numerical  $I(Q, 0)$ . We have further checked that this procedure yields identical results as the calculation of the total dynamical structure factor (in frequency space) convoluted with the experimental resolution. An example of this procedure is provided in Fig.S7.

---

[1] P. W. Fenimore, H. Frauenfelder, B. H. McMahon, and R. D. Young, Proc. Natl. Acad. Sci. U.S.A. **101**, 1440814413 (2004).

[2] S. Capaccioli, K. Ngai, S. Ancherbak, and A. Paciaroni, J. Phys. Chem. B **116**, 1745 (2012).

[3] W. Doster, S. Cusack, and W. Petry, Nature **337**, 754 (1989).

[4] W. Doster, Eur. Biophys. J. **37**, 591 (2008).

[5] J. Peters, J. Marion, F. Natali, E. K. Kats, and D. J. Bicout, J. Phys. Chem. B **121**, 6860 (2017).

[6] E. Cornicchi, S. Capponi, M. Marconi, G. Onori, and A. Paciaroni, Phil. Mag. **87**, 509 (2007).

[7] B. F. Rasmussen, A. M. Stock, D. Ringe, and G. A. Petsko, Nature **357**, 423424 (1992).

[8] Y. He, P. I. Ku, J. Knab, J. Chen, and A. Markelz, Phys. Rev. Lett. **101**, 178103 (2008).

[9] G. Schiro, C. Caronna, F. Natali, M. M. Koza, and A. Cupane, J. Phys. Chem. Lett. **2**, 2275 (2011).

[10] G. Schirò et al., Nat. Commun. **6** (2015).

[11] K. Wood et al., J. Am. Chem. Soc. **130**, 4586 (2008).

[12] H. Frauenfelder et al., Proc. Natl. Acad. Sci. U.S.A. **106**, 5129 (2009).

[13] U. Lehnert, V. Rèat, M. Weik, G. Zaccai, and C. Pfister, Biophys. J. **75**, 1945 (1998).

[14] A. Paciaroni, E. Cornicchi, M. Marconi, A. Orecchini, C. Petrillo, M. Haertlein, M. Moulin, and F. Sacchetti, J. R. Soc. Interface **6**, S635S640 (2009).

[15] A. Fernandez-Nieves, H. Wyss, J. Mattsson, and D. A. Weitz, *Microgel suspensions: fundamentals and applications* (John Wiley & Sons, 2011).

[16] M. Stieger, J. Pedersen, P. Lindner, and W. Richtering, Langmuir **20**, 7283 (2004).

[17] P. Yunker et al., Rep. Prog. Phys. **77**, 056601 (2014).

[18] F. Afrose, E. Nies, and H. Berghmans, J. Mol. Struct. **554**, 55 (2000).

[19] K. Van Durme, G. Van Assche, and B. Van Mele, Macromolecules **37**, 9596 (2004).

[20] E. Zaccarelli, M. Bertoldo, F. Natali, J. Ollivier, A. Orecchini, A. Paciaroni, and M. Zanatta, *Fast and slow dynamics in pnipam microgels* (2015), DOI:10.5291/ILL-DATA.9-11-1736.

[21] D. Paloli, P. S. Mohanty, J. J. Crassous, E. Zaccarelli, and P. Schurtenberger, Soft Matter **9**, 3000 (2013).

[22] I. Bischofberger and V. Trappe, Sci. Rep. **5**, 15520 (2015).

[23] Y. Ono and T. Shikata, J. Am. Chem. Soc. **128**, 10030 (2006).

[24] F. Sciortino, P. Gallo, P. Tartaglia, and S.-H. Chen, Phys. Rev. E **54**, 6331 (1996).

[25] S. Combet and J.-M. Zanotti, Phys. Chem. Chem. Phys. **14**, 4927 (2012).

[26] S.-H. Chen et al., Proc. Natl. Acad. Sci. U.S.A. **103**, 9012 (2006).

[27] W. Doster et al., Phys. Rev. Lett. **104**, 098101 (2010).

[28] P. Gallo, M. Rovere, and S.-H. Chen, J. Phys. Chem. Lett. **1**, 729 (2010).

[29] G. Camisasca, M. De Marzio, D. Corradini, and P. Gallo, J. Chem. Phys. **145**, 044503 (2016).

[30] L. A. Lyon and A. Fernandez-Nieves, Annu. Rev. Phys. Chem. **63**, 25 (2012).

[31] D. Vlassopoulos and M. Cloitre, Curr. Opin. Colloid Interface Sci. **19**, 561 (2014).

[32] J. L. F. Abascal, E. Sanz, R. G. Fernández, and C. Vega, J. Chem. Phys. **122**, 234511 (2005).

[33] J. L. F. Abascal and C. Vega, J. Chem. Phys. **123**, 234505 (2005).

[34] Z. Liu et al., Phys. Rev. Lett. **119**, 048101 (2017).

[35] E. Mamontov, V. Sharma, J. Borreguero, and M. Tyagi, J. Phys. Chem. B **120**, 3232 (2016).

[36] J. Smith, K. Kuczera, and M. Karplus, Proc. Natl. Acad. Sci. U.S.A. **87**, 1601 (1990).

[37] A. Paciaroni, S. Cinelli, and G. Onori, Biophysical journal **83**, 1157 (2002).

[38] P. Flory, J. Mark, and A. Abe, J. Am. Chem. Soc. **88**, 639 (1966).

[39] S. Pál et al., *Tackling Exascale Software Challenges in Molecular Dynamics Simulations with GROMACS* (Springer International Publishing, Cham, 2015), pp. 3–27.

[40] M. Abraham et al., SoftwareX **12**, 19 (2015).

[41] W. L. Jorgensen, D. S. Maxwell, and J. Tirado-Rives, J. Am. Chem. Soc. **118**, 11225 (1996).

[42] S. W. I. Siu, K. Pluhackova, and R. A. Beckmann, J. Chem. Theory Comput. **8**, 1459 (2012).

[43] G. Goret, B. Aoun, and E. Pellegrini, J. Chem. Inf. Model. **57**, 1 (2017).

[44] M. Seeber et al., J. Comput. Chem. **32**, 1183 (2011).

[45] W. Humphrey, A. Dalke, and K. Schulten, J. Mol. Graph. **14**, 33 (1996).